

Compound and Solid-Solution Formation in the System $\text{Li}_2\text{O}-\text{Nb}_2\text{O}_5-\text{TiO}_2$

M. E. VILLAFUERTE-CASTREJÓN, A. ARAGÓN-PIÑA,
R. VALENZUELA, AND A. R. WEST*

Instituto de Investigaciones en Materiales, Universidad Nacional Autónoma de México, Apartado Postal 70-360, México 04510, D.F.

Received January 27, 1986; in revised form January 22, 1987

A systematic study of compound and solid-solution formation in the system $\text{Li}_2\text{O}-\text{Nb}_2\text{O}_5-\text{TiO}_2$ has been made. Several solid-solution series, based on LiNbO_3 , LiNb_3O_8 , $\text{Li}_2\text{Nb}_{28}\text{O}_{71}$, Li_2TiO_3 , phase M, $\text{Li}_2\text{Ti}_3\text{O}_7$, and TiO_2 , have been characterized. In all cases, the principal solid-solution mechanism appears to involve stoichiometric formulae with constant overall cation content. One new phase, of approximate formula $\text{Li}_{13}\text{TiNb}_5\text{O}_{21}$, has been prepared. A subsolidus phase diagram for the ternary system is presented. © 1987 Academic Press, Inc.

Introduction

The title system contains a number of well-characterized binary compounds. Of these, LiNbO_3 is an important material with applications in optoelectronics (1-3); its properties may be modified by incorporating a certain amount of Ti^{4+} into the structure (4, 5). $\text{Li}_2\text{Ti}_3\text{O}_7$ has possible applications as a Li^+ ion-conducting solid electrolyte, especially at elevated temperatures (6, 7). TiO_2 has various applications, including use as an electrode material if its electronic characteristics can be modified suitably (8-12). Preliminary studies on the system $\text{Li}_2\text{O}-\text{Nb}_2\text{O}_5-\text{TiO}_2$ have led to the synthesis of various new materials, including extensive rutile solid solutions, $\text{Ti}_{1-4x}\text{Li}_x\text{Nb}_{3x}\text{O}_2$, $0 < x < 0.17$ (13), LiNb_3O_8

solid solutions, $\text{Li}_{1-x}\text{Nb}_{3-3x}\text{Ti}_{4x}\text{O}_8$, $0 < x \leq 0.06$ (13), Li_2TiO_3 solid solutions, $\text{Li}_{2+x}\text{Nb}_{3x}\text{Ti}_{1-4x}\text{O}_3$, $0 < x \leq 0.22$, which exhibit an ordering-disordering transition (14), and a new phase, M, $\text{Li}_{1+x}\text{Nb}_{1-x}\text{Ti}_x\text{O}_3$, $0.10 < x < 0.33$, with a distorted LiNbO_3 structure (15).

The three bounding binary systems have all been well-studied and phase diagrams are available for each. In the system $\text{Li}_2\text{O}-\text{Nb}_2\text{O}_5$, the most recent phase diagrams (16, 17) show the existence of the phases Li_3NbO_4 , LiNbO_3 with a range of stoichiometry from 50 to ~56.5 mole% Nb_2O_5 , LiNb_3O_8 , and $\text{Li}_2\text{Nb}_{28}\text{O}_{71}$. The phase diagram for the system $\text{Li}_2\text{O}-\text{TiO}_2$ (18) shows the phases Li_4TiO_4 , Li_2TiO_3 with a range of stoichiometry at high temperatures extending from ~44 to 66 mole% TiO_2 , $\text{Li}_4\text{Ti}_5\text{O}_{12}$, and $\text{Li}_2\text{Ti}_3\text{O}_7$ with a narrow range of stoichiometry between 74 and 76% TiO_2 . The phase diagram first reported for the system $\text{Nb}_2\text{O}_5-\text{TiO}_2$ (19) shows the formation of

* Permanent address: University of Aberdeen, Department of Chemistry, Meston Walk, Aberdeen AB9 2UE, UK.

Nb_2O_5 solid solutions containing up to 5 to 10% TiO_2 and the phases Nb_2TiO_7 , $\text{Nb}_6\text{TiO}_{17}$, and TiO_2 solid solutions containing up to ~15% Nb_2O_5 . In a more recent study of Nb_2O_5 -rich compositions (20), the phase $\text{Nb}_6\text{TiO}_{17}$ is replaced by the phase $\text{Nb}_{10}\text{Ti}_2\text{O}_{29}$, in accordance with crystallographic studies on the latter compound (21). The high-temperature phase, $\text{Nb}_6\text{Ti}_2\text{O}_{19}$, is also reported (20), with a lower limit of stability at 1425°C. Further modifications are made in the latest Nb_2O_5 - TiO_2 phase diagram (22). These show very little solid solution of TiO_2 in Nb_2O_5 but instead formation of the phase $\text{TiNb}_{24}\text{O}_{62}$ (23). However, no recognition of the phase $\text{Nb}_6\text{Ti}_2\text{O}_{19}$ (20) is made in this phase diagram (22).

Systematic studies on the ternary system Li_2O - Nb_2O_5 - TiO_2 have been limited to the three joins mentioned above, TiO_2 - LiNb_3O_8 (13), Li_2TiO_3 - Li_3NbO_4 (14), and Li_2TiO_3 - LiNbO_3 (15), and a study of LiNbO_3 solid solutions on the join LiNbO_3 - TiO_2 (24). In this latter study, a partial phase diagram for the join was given, together with the results on the composition dependence of the lattice parameters and ferroelectric Curie temperature of the LiNbO_3 solid solutions. The present paper reports the results of a comprehensive study of compound and solid-solution formation in the ternary system Li_2O - Nb_2O_5 - TiO_2 for all compositions with the exception of those rich in Li_2O .

Experimental

Starting materials were Li_2CO_3 (reagent grade), Nb_2O_5 (99.9%, Aldrich), and TiO_2 (99.2%, Baker). Mixtures totalling 5 to 10 g were prepared by weighing, mixing into a paste with acetone in an agate mortar, drying, and firing in Pt crucibles or Au foil boats; Au was used for compositions containing >50% Li_2O . The mixtures were fired in electric muffle furnaces whose tem-

peratures were controlled and measured to $\pm 30^\circ\text{C}$. Initial firing was at 600 to 700°C for a few hours to expel CO_2 followed by $\sim 900^\circ\text{C}$ for 12–48 hr. After grinding, the samples were finally fired at temperatures in the range 900 to 1200°C for 24–72 hr, depending on composition. Careful checks were made to ensure that lithia loss by evaporation did not occur to an appreciable extent, especially for the more lithia-rich compositions.

The products of reaction were identified by X-ray powder diffraction using a Siemens D500 diffractometer, CuK_α radiation.

Results

The results of heating experiments on more than 130 compositions, given in an unpublished table,¹ were used to construct the phase diagram given in Fig. 1. This diagram pertains to subsolidus temperatures of ca. 1050 to 1150°C. The phase diagram at lower temperatures is expected to show certain differences, as discussed later. At higher temperatures, 1200 to 1300°C, most compositions are expected to show at least partial melting. The exceptions are those compositions close to the Nb_2O_5 - TiO_2 join, most of which are expected to melt at considerably higher temperatures. No systematic study of the melting behavior has been made, apart from that reported previously for the binary joins Li_2TiO_3 - Li_3NbO_4 (14) and Li_2TiO_3 - LiNbO_3 (15). The various crystalline single-phase regions in the ternary system are now discussed in turn.

LiNbO₃ Solid Solutions

LiNbO_3 is an unusual material in that it exists on the join Li_2O - Nb_2O_5 as a solid-solution series over the composition range 50 to 56.5% Nb_2O_5 (2, 25), with a congruently melting composition at 51.4% Nb_2O_5 .

¹ Available from the authors on request.

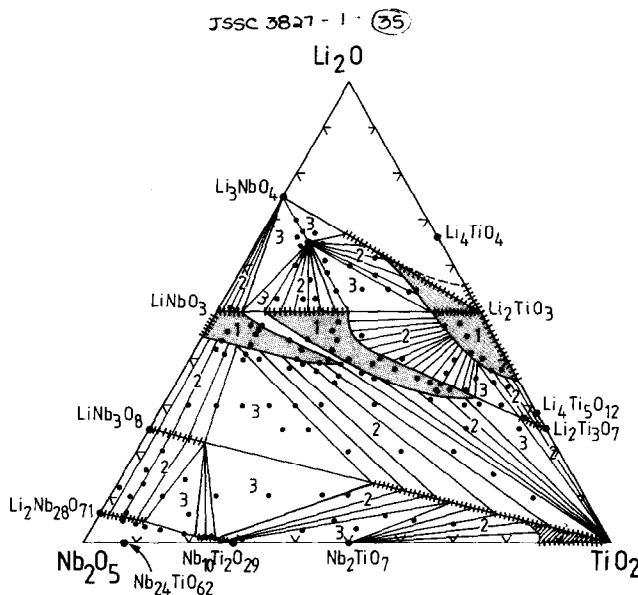


FIG. 1. Phase diagram for the system $\text{Li}_2\text{O}-\text{Nb}_2\text{O}_5-\text{TiO}_2$ at ca. 1100°C (in mole%). The compositions studied are marked with solid circles. Compositions to the lithia-rich side of the join $\text{Li}_3\text{NbO}_4-\text{Li}_2\text{TiO}_3$ were not studied. Studies in the Nb_2O_5 -rich corner were inconclusive and these results have been omitted.

Limited ranges of LiNbO_3 solid solutions have been prepared on the joins $\text{LiNbO}_3-\text{Li}_2\text{TiO}_3$ (15) and $\text{LiNbO}_3-\text{TiO}_2$ (24). Our new results show that, in the ternary system, an extensive, wedge-shaped solid-solution area forms (Fig. 1). This solid solution is most extensive in the direction of the hypothetical compound " $\text{Li}_2\text{Ti}_4\text{O}_9$,"

as emphasized in Fig. 2. On the join $\text{LiNbO}_3-\text{Li}_2\text{Ti}_4\text{O}_9$, the solid-solution mechanism is such that the total cation content remains constant, viz.,



This gives the solid-solution formula Li_{1-x}

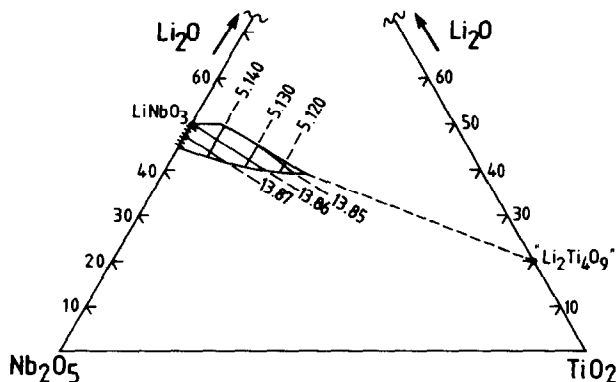


FIG. 2. The LiNbO_3 solid-solution field (in mole%), most extensive in the direction of the hypothetical compound " $\text{Li}_2\text{Ti}_4\text{O}_9$." Contours of constant lattice parameter are marked for a (5.140 to 5.120 Å) and c (13.85 to 13.87 Å).

$\text{Nb}_{1-3x}\text{Ti}_{4x}\text{O}_3$. The range of x is found experimentally to be $0 < x < 0.10$.

The lattice parameters of a selection of LiNbO_3 solid-solution compositions have been measured and used to determine the contours of constant lattice parameter content, as indicated in Fig. 2. The hexagonal a parameter shows a gradual decrease with increasing TiO_2 content. The c parameter behaves quite differently and the contours run approximately parallel to the LiNbO_3 – TiO_2 join.

The results reported in (24) were for the join LiNbO_3 – TiO_2 and are largely consistent with our studies on the complete area of LiNbO_3 solid solutions. From Figs. 1 and 2, the LiNbO_3 solid solutions on the join LiNbO_3 – TiO_2 extend to the approximate composition 40 mole% Li_2O , 40% Nb_2O_5 , 20% TiO_2 . When these solid solutions are written in the form $\text{LiNbO}_3 \cdot x\text{TiO}_2$, the 40:40:20 composition corresponds to a value of x of 0.25. The limiting value of x given in (24) is somewhat less, i.e., 0.205.

LiNb₃O₈ Solid Solutions

These are described in (13) and have not been studied further. They are shown in Fig. 1 as a hatched line extending part way along the join LiNb_3O_8 – TiO_2 . Again, it should be noted that these solid solutions have a replacement mechanism which retains a constant total cation content.

Li₂Nb₂₈O₇₁ Solid Solutions

There was some evidence to suggest that $\text{Li}_2\text{Nb}_{28}\text{O}_{71}$ forms a limited range of solid solutions in the ternary system. The results are consistent with the same replacement mechanism, giving constant overall cation content, that was found for the solid-solution series involving LiNbO_3 and LiNb_3O_8 described above and for the solid solutions of TiO_2 and $\text{Li}_2\text{Ti}_3\text{O}_7$ discussed later. For the $\text{Li}_2\text{Nb}_{28}\text{O}_{71}$ solid solutions, this mechanism gives rise to the solid-solution formula $\text{Li}_{2-x}\text{Nb}_{28-3x}\text{Ti}_{4x}\text{O}_{71}$ and

for which the experimental range of x values is $0 < x < 0.43$. The theoretical limit for this solid-solution series occurs when $x = 2$ and corresponds to the composition of the hypothetical phase “ $11\text{Nb}_2\text{O}_5 \cdot 8\text{TiO}_2$.”

Rutile Solid Solutions

Extensive rutile solid solutions on the join TiO_2 – LiNb_3O_8 were reported in (13) and a more limited range on the join Nb_2O_5 – TiO_2 in (19). These two series probably link up to form a limited area of ternary solid solutions, bounded approximately by the dashed line shown in Fig. 1, although direct experiments to confirm this have not been made.

Li₂Ti₃O₇ Solid Solutions

A limited range of $\text{Li}_2\text{Ti}_3\text{O}_7$ solid solutions forms with the probable replacement mechanism $4\text{Ti}^{4+} \rightleftharpoons \text{Li}^+ + 3\text{Nb}^{5+}$ and formula $\text{Li}_{2+x}\text{Nb}_{3x}\text{Ti}_{3-4x}\text{O}_7$, $0 < x \leq 0.08$. The hypothetical end-member of this series is the nonexistent phase “ $11\text{Li}_2\text{O} \cdot 9\text{Nb}_2\text{O}_5$.”

Li₂TiO₃ Solid Solutions

An extensive area of ternary Li_2TiO_3 solid solutions forms at high temperatures, in agreement with previous studies on the joins Li_2O – TiO_2 (18), Li_2TiO_3 – Li_3NbO_4 (14), and Li_2TiO_3 – LiNbO_3 (15). Detailed studies on the variation of the low \rightleftharpoons high polymorphic transition temperature with composition have not been made for the ternary system but could be estimated by combining data for the various joins mentioned above.

Phase M Solid Solutions

Phase M is the solid-solution phase $\text{Li}_{1+x}\text{Nb}_{1-x}\text{Ti}_{1+x}\text{O}_3$, $0.10 < x < 0.33$, first prepared on the join Li_2TiO_3 – LiNbO_3 (15). Studies on the ternary system show it to form a very extensive, wedge-shaped area of ternary solid solutions. These solid solutions may also, in large part, be derived by the replacement mechanism $\text{Li}^+ + 3\text{Nb}^{5+}$

$\rightleftharpoons 4\text{Ti}^{4+}$; for instance, one edge of the solid-solution field runs parallel with the Li₂Ti₃O₇ solid solutions described above. Structural information on these solid solutions is unfortunately lacking since, as yet, we have been unable to prepare single crystals of a size suitable for X-ray work. At the LiNbO₃-rich limit, the powder X-ray pattern of the solid solutions is quite similar to that of LiNbO₃ and hence a strong structural similarity between the M solid solutions and LiNbO₃ is suspected. With increasing Li₂TiO₃/TiO₂ content, major but apparently continuous changes in the X-ray powder patterns occur, as depicted for a selection of compositions in Fig. 3. Since the changes are large, it is possible that a series of structurally related phases exists, rather than a single homogeneous solid-solution series.

Phase C, "Li₁₃TiNb₅O₂₁"

This is a new lithia-rich phase stable only at high temperatures, $\approx 900^\circ\text{C}$. Its composi-

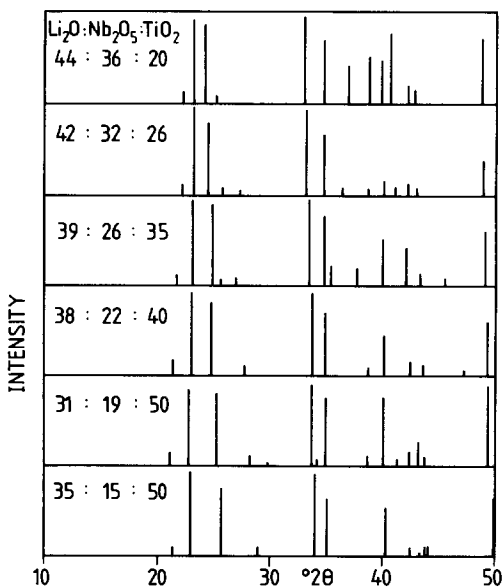


FIG. 3. A selection of X-ray line diagrams for different phase M solid-solution compositions. For each, the composition is given in terms of the oxide molar ratio.

tion has not been determined with certainty due to (i) problems of lithia volatilization on heating lithia-rich compositions for extended periods $>1000^\circ\text{C}$ and (ii) the slow rate of formation of this new phase. Its composition is most likely to be $65\text{Li}_2\text{O} \cdot 10\text{TiO}_2 \cdot 25\text{Nb}_2\text{O}_5$ or $\text{Li}_{13}\text{TiNb}_5\text{O}_{21}$. In order to reduce lithia loss, pelleted samples were immersed in presintered powder of the same composition and wrapped in Pt foil bags; after heat treatments the pellets were separated from the surrounding powder and analyzed by X-ray powder diffraction. The decomposition of phase C at temperatures $\approx 900^\circ\text{C}$ takes place relatively slowly and hence phase C may be quenched readily to ambient temperatures, where it is kinetically stable. Unindexed X-ray powder data are given in Table I.

Subsolidus Compatibility Relations at $\sim 1100^\circ\text{C}$

Apart from the eight ternary phases/solid-solution series outlined above, all remaining compositions on the lithia-deficient side of the join Li₃NbO₄–Li₂TiO₃ give a mixture of either two or three of these eight phases, as indicated in Fig. 1. The Nb₂O₅-rich corner has not been determined in detail and is left blank.

Subsolidus Compatibility Relations at $\leq 950^\circ\text{C}$

Detailed studies of the phase relations at lower temperatures have not been made but some differences must inevitably be present. Thus,

—Li₄Ti₅O₁₂ is a thermodynamically stable phase at temperatures $<1025^\circ\text{C}$ and should therefore be observed in some ternary compositions.

—Li₂Ti₃O₇ is unstable $\leq 950^\circ\text{C}$ and should be absent from the diagram, unless the effect of the solid-solution formation is to stabilize Li₂Ti₃O₇ to much lower temperatures.

TABLE I
X-RAY POWDER
DIFFRACTION DATA FOR
PHASE C, "Li₁₃TiNb₅O₂₁"

d^a (Å)	I
6.524	23
6.159	14
4.477	4
3.761	5
3.691	31
3.487	19
3.261	20
2.882	18
2.781	5
2.632	7
2.439	17
2.381	4
2.284	2
2.238	3
2.110	100
2.047	2
1.954	5
1.880	4
1.807	3
1.773	2
1.571	6
1.487	41
1.448	4
1.273	2
1.217	5

^a Internal standard for d measurements was NaCl.

—The Li₂TiO₃ solid solutions are considerably less extensive at lower temperatures, below the temperature of the low \rightleftharpoons high transition.

—Phase C is unstable $\leq 950^\circ\text{C}$ and should be absent from the diagram.

Acknowledgments

We thank the British Council for supporting the Aberdeen–Mexico collaboration programme and L. Baños for help with the X-ray diffraction analyses.

References

1. B. T. MATTHIAS AND J. P. REMEIKA, *Phys. Rev.* **76**, 1886 (1949).
2. P. LERNER, C. LEGRAS, AND J. P. DUMAS, *J. Cryst. Growth* **3/4**, 231 (1968).
3. G. E. PETERSON, A. A. BALLMAN, P. V. LENZO, AND P. M. BRIDENBAUGH, *Appl. Phys. Lett.* **5**, 62 (1964).
4. R. V. SCHMIDT AND I. P. KAMINOW, *Appl. Phys. Lett.* **25**, 458 (1974).
5. K. SUGII, M. FUKUMA, AND H. IWASAKI, *J. Mater. Sci.* **13**, 523 (1978).
6. J. B. BOYCE AND J. C. MIKKELSEN, JR., *Solid State Commun.* **31**, 741 (1979).
7. J. B. BOYCE, J. C. MIKKELSEN, JR., AND B. A. HUBERMAN, *Solid State Commun.* **29**, 507 (1979).
8. M. ITAKURA, N. NÜZEKI, H. TOYODA, AND H. IWASAKI, *Japan. J. Appl. Phys.* **6**, 311 (1967).
9. O. W. JOHNSON AND G. R. MILLER, *Ceram. Bull.* **56**, 706 (1977).
10. A. FUJISHIMA AND K. HONDA, *Nature (London)* **238**, 38 (1972).
11. D. W. MURPHY, R. J. CAVA, S. M. ZAHURAK, AND A. SANTORO, *Solid State Ionics* **9/10**, 413 (1983).
12. L. BROHAN AND R. MARCHAND, *Solid State Ionics* **9/10**, 419 (1983).
13. J. A. GARCÍA, M. E. VILLAFUERTE-CASTREJÓN, J. ANDRADE, R. VALENZUELA, AND A. R. WEST, *Mater. Res. Bull.* **19**, 649–654 (1984).
14. A. ARAGÓN-PIÑA, M. E. VILLAFUERTE-CASTREJÓN, R. VALENZUELA, AND A. R. WEST, *J. Mater. Sci. Lett.* **3**, 893 (1984).
15. M. E. VILLAFUERTE-CASTREJÓN, J. A. GARCÍA, E. CISNEROS, R. VALENZUELA, AND A. R. WEST, *Trans. J. Brit. Ceram. Soc.* **83**, 143 (1984).
16. R. S. ROTH, H. S. PARKER, W. S. BROWER, AND J. L. WARING, in "Fast Ion Transport in Solids, Solid State Batteries and Devices" (W. van Gool, Ed.), p. 217, North-Holland, Amsterdam (1973).
17. L. O. SVAASAND, M. ERIKSRUD, A. P. GRANDE, AND F. MO, *J. Cryst. Growth* **18**, 179 (1973).
18. G. IZQUIERDO AND A. R. WEST, *Mater. Res. Bull.* **15**, 1655 (1980).
19. R. S. ROTH AND L. W. COUGHANOUR, *J. Res. Nat. Bur. Stand.* **55**, 211 (1955).
20. A. JONGEJAN AND A. L. WILKINS, *J. Less-Common Met.* **19**, 186 (1969).
21. A. D. WADSLEY, *Acta Crystallogr.* **14**, 664 (1961).
22. R. S. ROTH, *Prog. Solid State Chem.* **13**(2), 159–192 (1980).
23. R. S. ROTH AND A. D. WADSLEY, *Acta Crystallogr.* **18**(4), 724–730 (1965).
24. B. GUENAI, M. BAUDET, M. MINIER, AND M. LE CUN, *Mater. Res. Bull.* **16**, 643 (1981).
25. J. R. CARRUTHERS, G. E. PETERSON, M. GRASSO, AND P. M. BRIDENBAUGH, *J. Appl. Phys.* **42**, 1846 (1971).